



Article scientifique

Article

2012

Published version

Open Access

This is the published version of the publication, made available in accordance with the publisher's policy.

The Glucocorticoid-induced leucine zipper (GILZ) Is essential for spermatogonial survival and spermatogenesis

Romero, Yannick; Vuandaba, Mavunza Livia; Suarez, P; Grey, C; Calvel, Pierre; Conne, Béatrice; Pearce, D; de Massy, B; Hummler, E; Nef, Serge

How to cite

ROMERO, Yannick et al. The Glucocorticoid-induced leucine zipper (GILZ) Is essential for spermatogonial survival and spermatogenesis. In: Sexual development, 2012, vol. 6, n° 4, p. 169–177. doi: 10.1159/000338415

This publication URL: <https://archive-ouverte.unige.ch/unige:27978>

Publication DOI: [10.1159/000338415](https://doi.org/10.1159/000338415)

The Glucocorticoid-Induced Leucine Zipper (GILZ) Is Essential for Spermatogonial Survival and Spermatogenesis

Y. Romero^a M. Vuandaba^a P. Suarez^b C. Grey^c P. Calvel^a B. Conne^a D. Pearce^d
B. de Massy^c E. Hummler^b S. Nef^a

^aDepartment of Genetic Medicine and Development, University of Geneva Medical School, Geneva, ^bPharmacology and Toxicology Department, University of Lausanne, Lausanne, Switzerland; ^cInstitut de Génétique Humaine, IGH – CNRS, Montpellier, France; ^dDiabetes Center, University of California, San Francisco, Calif., USA

Key Words

GILZ · Spermatogenesis · Spermatogonia · *Tsc22d3*

Abstract

Spermatogenesis relies on the precise regulation of the self-renewal and differentiation of spermatogonia to provide a continuous supply of differentiating germ cells. The understanding of the cellular pathways regulating this equilibrium remains unfortunately incomplete. This investigation aimed to elucidate the testicular and ovarian functions of the glucocorticoid-induced leucine zipper protein (GILZ) encoded by the X-linked *Tsc22d3* (*Gilz*) gene. We found that GILZ is specifically expressed in the cytoplasm of proliferating spermatogonia and preleptotene spermatocytes. While *Gilz* mutant female mice were fully fertile, constitutive or male germ cell-specific ablation of *Gilz* led to sterility due to a complete absence of post-meiotic germ cells and mature spermatozoa. Alterations were observed as early as postnatal day 5 during the first spermatogenic wave and included extensive apoptosis at the spermatogonial level and meiotic arrest in the mid-late zygotene stage. Overall, these data emphasize the essential role played by GILZ in mediating spermatogonial survival and spermatogenesis. Copyright © 2012 S. Karger AG, Basel

Spermatogenesis is a complex biological process that involves the proliferation and differentiation of diploid spermatogonia into mature haploid spermatozoa. During the first phase of this process, spermatogonial stem cells (SSCs) enter a series of mitotic divisions which give rise to a pool of differentiated B spermatogonia, the precursors of the meiotic cells. The primary spermatocytes then undergo 2 meiotic divisions to generate haploid spermatids, which in turn differentiate into spermatozoa during a phase known as spermiogenesis.

In mice, the SSCs, the majority of which is believed to be A-single (A_s) spermatogonia, are located on the basement membrane of the seminiferous tubules. During the first phase of spermatogenesis, A_s spermatogonia enter a series of mitotic divisions giving rise first to pairs of spermatogonia (A_{pr}) that divide further to form a chain of up to 32 aligned spermatogonia (A_{al}). These subsequently differentiate into A1 spermatogonia, then further divide into A2, A3, A4, In (intermediate) and B spermatogonia, the precursors of the meiotic cells [for a review, see de Rooij and de Boer, 2003].

SSC self-renewal and differentiation is essential to provide a continuous supply of differentiating germ cells and must be strictly regulated to prevent SSC exhaustion.

KARGER

Fax +41 61 306 12 34
E-Mail karger@karger.ch
www.karger.com

© 2012 S. Karger AG, Basel
1661-5425/12/0000-0000\$38.00/0

Accessible online at:
www.karger.com/sxd

Serge Nef
Department of Genetic Medicine and Development
University of Geneva Medical School
1 rue Michel-Servet, CH-1211 Geneva 4 (Switzerland)
Tel. +41 22 379 5193, E-Mail serge.nef@unige.ch

Several factors essential for spermatogonial development have been identified and include both extrinsic factors produced by Sertoli cells, such as glial cell-derived neurotrophic factor (GDNF), fibroblast growth factor 2 (FGF2) and bone morphogenetic protein 4 (BMP4), as well as intrinsic spermatogonial factors, including Zinc finger and BTB domain-containing 16 (ZBTB16/PLZF) and ets variant gene 5 (ETV5/ERM) [for reviews, see Zhou and Griswold, 2008; de Rooij, 2009]. However, our understanding of the molecular pathways regulating the fine equilibrium between self-renewal, proliferation, differentiation and apoptosis of male germ cells is still incomplete, and it has become clear that additional factors must be involved.

The glucocorticoid-induced leucine zipper (GILZ) is a 17-kDa leucine zipper protein of the transforming growth factor (TGF) β -stimulated clone 22 domain (TSC22D) family, encoded by the X-linked *Tsc22d3* gene. It is expressed in various tissues including brain, kidney, liver, skeletal muscle, and immune tissues (e.g. lymphocytes from the thymus, spleen and lymph nodes) [for more details, see D'Adamio et al., 1997]. GILZ has been proposed to function as a key mediator of the anti-inflammatory and immunosuppressive effects of glucocorticoids [Krzysiek, 2010]. In addition, GILZ has also been implicated in the control of cell survival, proliferation and differentiation [D'Adamio et al., 1997; Delfino et al., 2004; Ayroldi et al., 2007; Redjimi et al., 2009] as well as numerous other functions, such as adipogenesis [Shi et al., 2003], renal sodium transport [Soundararajan et al., 2005] and dendritic cell function [Cohen et al., 2006]. GILZ was shown to interact directly with multiple proteins, including Ras [Ayroldi et al., 2007] and Raf [Ayroldi et al., 2002], and to inhibit downstream signals such as ERK, AKT, retinoblastoma protein (Rb) phosphorylation, and cyclin D1 expression [Ayroldi et al., 2002, 2007; Soundararajan et al., 2005]. In fact, the broad expression profile of GILZ, coupled with its large spectrum of reported activities, suggests that its function may differ significantly depending on the cell type, tissue or physiological system.

Interestingly, microarray expression profiles in male germ cells suggest that *Gilz* transcripts are present at high levels in mouse spermatogonia [Chalmel et al., 2007; Lardenois et al., 2010]. In order to investigate the function of GILZ in male and female reproductive systems, we first analyzed its expression in the developing testis and then used gene-targeted deletion in mice to assess its role in both the testis and the ovary.

Material and Methods

Animals

A *Gilz*^{lox} allele was generated by inserting 2 Lox sites between exons 3 to 6, the first 4 coding exons of the *Tsc22d3* gene [Suarez et al., in press]. Ablation of these 4 exons resulted in complete absence of *Gilz* transcripts. *Gilz*^{lox} mice, *Ddx4:Cre (Mvh:Cre)* mice and *Amh:Cre* mice were genotyped as described [Lecureuil et al., 2002; Gallardo et al., 2007; Suarez et al., in press]. To achieve selective inactivation of *Gilz* in germ cells, we mated transgenic male mice expressing Cre recombinase under the control of the *Mvh* promoter with female mice carrying 2 floxed *Gilz* alleles in order to generate 50% *Ddx4:Cre;Gilz*^{fx/y} and 50% *Gilz*^{fx/y} male mice. These males were used to study the depletion of GILZ in the germline. On the other hand, *Gilz*^{fx/y} males were mated with *Ddx4:Cre;Gilz*^{fx/wt} females in order to produce *Ddx4:Cre;Gilz*^{fx/fx} females as well as *Gilz*^{fx/fx} and *Ddx4:Cre;Gilz*^{fx/wt} control littermates to assess the reproductive phenotype of mice specifically lacking GILZ in female germ cells. Selective inactivation of *Gilz* in Sertoli cells was obtained by crossing the *Amh:Cre* transgenic mice with the *Gilz*^{fx} mice. The genetic background of these mice was mixed, mainly C57/BL6N and SV129/EV. Animals were housed and cared for according to the ethical guidelines of the Direction Générale de la Santé of the Canton de Genève (experimentation ID: 1061/3805/0).

Sperm Analysis

Epididymal sperm count was performed with sperm extracted from the caudal epididymis and ductus deferens of adult, postnatal day (P)80 male mice as previously described [Romero et al., 2011].

Histology and Immunohistochemistry

Tissues were fixed overnight either in 4% paraformaldehyde or in Bouin's fixative and embedded in paraffin. Five- μ m sections were stained with haematoxylin and eosin (H&E) or processed for immunohistochemistry. For immunohistochemistry, paraformaldehyde-fixed sections were incubated overnight at 4°C with the following antibodies: anti-AMH (Santa Cruz Biotechnology, sc-9053, 1:500), anti-pH3(Ser10) (Millipore, Cat. No. 06-570, 1:500), anti- γ H2AX (Calbiochem, Cat. No. dr-1017, 1:500), anti-H3K9me3 (Millipore, Cat. No. 07-523, 1:500), and rabbit anti-GILZ (gift from D. Pearce, 1:500 [Soundararajan et al., 2007]). For fluorescent staining, Alexa-conjugated secondary antibodies (Invitrogen) were used for signal detection, and sections were counterstained using DAPI. All images were obtained with a Zeiss AxioScope microscope and processed using the AxioVision LE software.

Apoptosis Assays

Apoptotic assays were performed by TdT-mediated X-dUTP nick end labelling (TUNEL) reactions using the Apoptag kit (Millipore), stained with either DAB chromogen and counterstained with eosin or with Permanent Red, or anti-digoxigenin coupled to fluorescein and counterstained with DAPI. The percentage of apoptotic, TUNEL-positive cells within seminiferous tubules was expressed as the average number of apoptotic cells within 20 seminiferous tubules. A minimum of 100 seminiferous tubules were counted per testis (5 sections/testis) and at least 3 animals per genotype and age were investigated.

Proliferation Assays

Proliferation assays were performed by assessing Ki-67 staining of paraffin-embedded sections at different ages, coupled with immunostaining using GCNA antibodies. The germ cell proliferation rate was determined by counting double-positive cells for Ki-67 and GCNA. A minimum of 100 seminiferous tubules were counted per testis (5 sections/ testis) and at least 3 animals per genotype and developmental stage were analyzed.

Chromosome Spread Preparation and Immunostaining

Spermatocyte nuclear spreads were prepared and stained as previously described [Grad et al., 2010]. The primary antibodies used were: guinea pig anti-SYCP3 (gift from C. Heyting, 1:25,000), mouse anti- γ H2AX (Upstate, Cat. No. 05-636, 1:25,000) and rabbit anti-DMC1 (Santa Cruz Biotechnology, H100, 1:200). Secondary antibodies were Alexa Fluor 488 and Alexa Fluor 594 conjugates (Molecular Probes). Digital images were obtained by using a cooled CCD camera, Coolsnap HQ (Photometrics), coupled to a Leica DMRA2 microscope using the same exposure time for all acquisitions. Each colour signal was acquired as a black-and-white image using appropriate filter sets and was merged with Photoshop Imaging software.

Male Fertility Tests

A group of 3 *Gilz* ^{Δ /y} mutant males, and a group of 3 *Gilz*^{wt/y} control males, were each bred with 2 wild-type C57/Bl6J females for a period of 3 months. The number of litters and pups per litter were recorded at weaning.

Statistical Analysis

Results of a representative experiment are shown and are expressed as means \pm SEM of n experiments. The nonparametric unpaired t test was used for statistical analysis. Differences were considered statistically significant if $p < 0.05$.

Results

Specific Expression of *Gilz* in Proliferating Spermatogonia and Preleptotene Spermatocytes

Available microarray data revealed that the *Gilz* gene is expressed in both the testis and the adult ovary [Chalmel et al., 2007; Lardenois et al., 2010]. Within the testis, *Gilz* transcripts were present at high levels in A and B spermatogonia, and to a lesser extent in Sertoli cells (online suppl. fig. 1; for all online supplementary material, see www.karger.com/doi/10.1159/000338415). Double immunofluorescence assays confirmed that GILZ is specifically localized in the cytoplasm of spermatogonia in the developing testis at birth (P0), P5 and P10 (fig. 1A–I). In the adult testis, GILZ protein was strongly detected in the cytoplasm of A and B spermatogonia, as well as in preleptotene spermatocytes (fig. 1J–O). No signal was detected in the somatic cells of either prepubertal or adult testis (online suppl. fig. 2 and data

not shown). In female mice, no expression of the GILZ protein was detected by immunofluorescence in the adult ovary (data not shown).

Constitutive Deletion of *Gilz* Results in Male Infertility

To investigate the functional relevance of GILZ in mice, we generated constitutive *Gilz* ^{Δ /y} males and *Gilz* ^{Δ / Δ} females by crossing mice containing a conditional *Gilz* allele (*Gilz*^{fx}) [Suarez et al., in press] with a germ cell-specific (*Ddx4*) promoter-driven transgenic Cre line [Gallardo et al., 2007]. More precisely, male mice carrying a *Gilz* floxed allele (*Gilz*^{fx/y}) were intercrossed with transgenic females expressing the Cre-recombinase under the control of the *Ddx4* promoter (*Gilz*^{fx/wt};*Ddx4:Cre*) to generate constitutive *Gilz* ^{Δ /y} males and *Gilz* ^{Δ / Δ} females as well as *Gilz*^{fx/y} and *Gilz*^{fx/fx} control animals. Immunofluorescence of P5 testis confirmed GILZ expression in control *Gilz*^{fx/y}, but not in *Gilz* ^{Δ /y} testes, indicating that gene expression was completely ablated in mutant mice (online suppl. fig. 3). *Gilz* ^{Δ / Δ} mutant female mice were viable, fertile and exhibited normal oestrous cyclicity, oocyte development and maturation, parturition frequency and litter size (online suppl. fig. 4). Similarly, *Gilz* ^{Δ /y} males were viable, grew to adulthood normally and appeared to have normal sexual behaviour and external genitalia when compared to control littermates. However, P80 adult testes lacking *Gilz* showed a significant (~80%) mass reduction compared to control *Gilz*^{fx/y} males (fig. 2A, B). Sperm count analysis revealed that no spermatozoa were present in P80 *Gilz* ^{Δ /y} caudal epididymides, whereas normal sperm counts were found for control littermates (fig. 2F). Histological analysis of *Gilz* ^{Δ /y} mice confirmed the complete absence of spermatozoa in the testes (fig. 2D) and epididymal ducts, whereas numerous exfoliated germ cells were found in the lumen of mutant epididymides (data not shown). *Gilz* ^{Δ /y} mutant testes showed features characteristic of a disorganized seminiferous epithelium, such as vacuolization, germ cells loss, Sertoli-cells-only tubules and interstitium hyperplasia (fig. 2C, D, G–N). Consistent with these multiple defects, mutant males were unable to produce offspring when mated with wild-type females [Suarez et al., in press and data not shown].

Germ Cell-Specific Deletion of *Gilz* in Conditional *Ddx4:Cre*;*GILZ*^{fx/y} Testes

The specific expression of GILZ in spermatogonia and early spermatocytes suggests that the infertility phenotype observed in male mutants might result from a germ

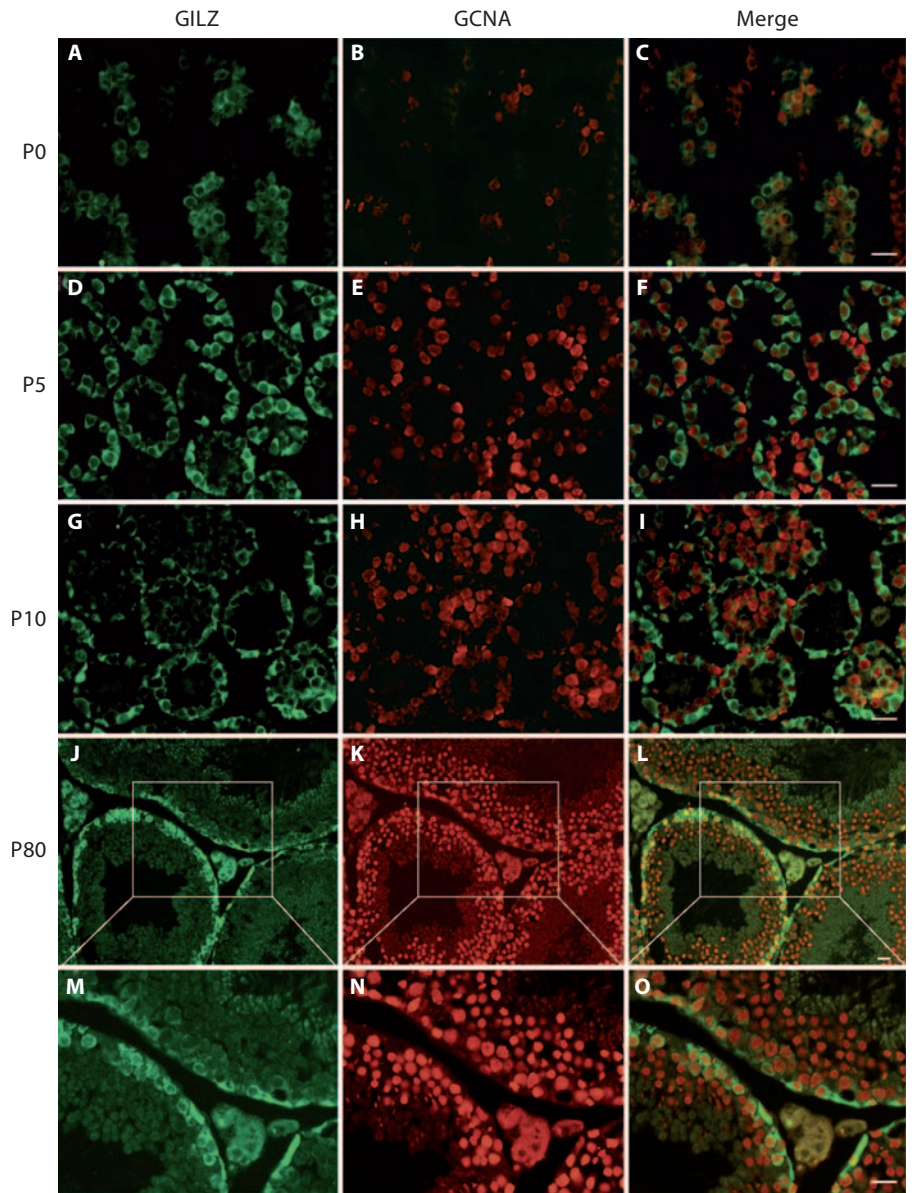


Fig. 1. Spatiotemporal expression of GILZ during testicular development in wild type mice. Double immunolabelling for GILZ (green) and the germ cell marker GCNA (red) in the testis at various developmental stages: postnatal day (P) 0 (A–C), P5 (D–F), P10 (G–I) and adult P80 (J–O). A merged image of green and red is shown in the right panel. At P0 and P5, GILZ is expressed in the cytoplasm of developing spermatogonia. At P10, at the onset of meiosis, GILZ is present in the cytoplasm of B spermatogonia and a faint signal is detected in early prophase I spermatocytes localised in the centre of the seminiferous tubule. In adult testis, GILZ is expressed at the periphery of the tubule, showing expression in A spermatogonia (flattened basal pole), B spermatogonia, and in early spermatocytes (round cells). Scale bars = 20 μ m.

cell-specific defect. To test this hypothesis, we specifically deleted *Gilz* in either Sertoli cells using a well-known and efficient Sertoli-specific Cre line, the *Amh:Cre* transgene [Lecureuil et al., 2002], or in male germ cells using the *Ddx4:Cre* transgenic line [Gallardo et al., 2007]. Mice with a specific deletion of *Gilz* in Sertoli cells (*Amh:Cre;Gilz^{fx/y}*) were viable and fertile, with normal reproductive parameters, including typical testicular histology, testis size and sperm production (online suppl. fig. 5A–F). We then investigated the functional relevance of GILZ when specifically deleted in germ cells during

spermatogenesis. Surprisingly, when *Ddx4:Cre;Gilz^{wt/y}* males were mated with *Gilz^{fx/fx}* females, the Mendelian ratio observed for the *Ddx4:Cre;Gilz^{fx/y}* progeny was far less than the expected 25% ratio. This phenomenon could be explained by the leakiness of the *Ddx4:Cre* transgene during the first zygotic divisions, a well-known phenomenon that might have led to the generation of constitutive instead of germ cell-specific mutants. Nevertheless, the few available *Ddx4:Cre;Gilz^{fx/y}* mice exhibited a reproductive phenotype identical to that observed in the constitutive *Gilz^{Δy}* mutants. It included reduced testis size,

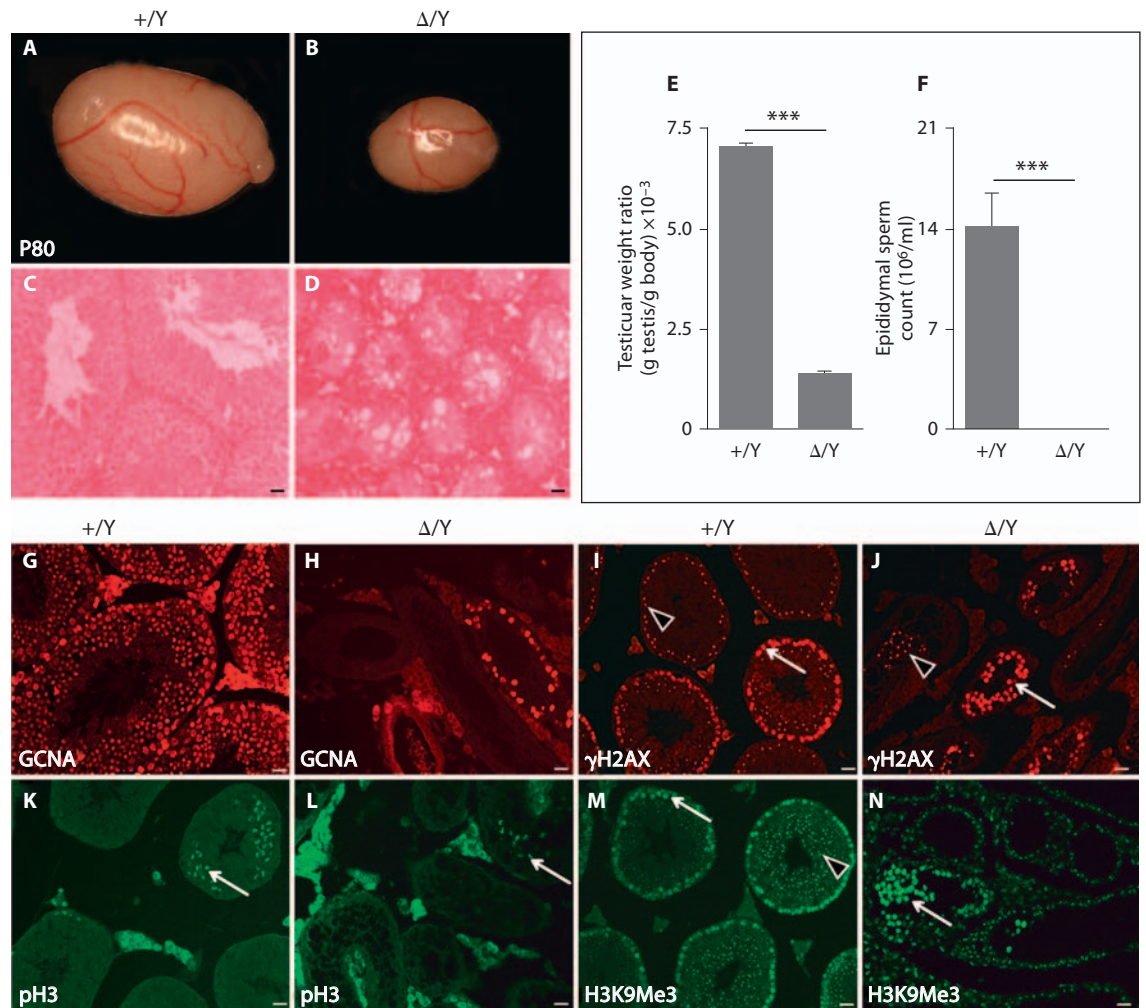


Fig. 2. Reduction in testis size and absence of spermatozoa in *Gilz*^{Δ/y} mutant mice. P80 adult testes from *Gilz*^{Δ/y} (Δ/Y, n = 11) (B) mice showed an 80% reduction in weight (E) compared to control (+/Y, n = 6) littermates (A). H&E staining of testes sections (C, D) revealed complete absence of mature spermatozoa and elongated spermatids in Δ/Y testes. F Sperm count analysis revealed a complete absence of epididymal sperm in Δ/Y mutant animals. G, H Immunostaining using GCNA antibody revealed a drastic reduction in the number of germ cells present in mutant seminiferous tubules (H) compared to +/Y tubules (G). I, J Anti-γH2AX staining revealed the reduced presence of early meiotic spermatocytes (whole nucleus staining, arrows) and few sparse pachytene spermatocytes (punctate staining, arrowheads) within Δ/Y testis (J) compared to wild type (I). Few metaphasic cells are also present in *Gilz* mutants as shown by histone H3Ser10 phosphorylated (pH3) positive cells (compare staining in K and L). M, N Sex chromatin of round spermatids is detected by punctate H3K9Me3 staining in control tubules (M, arrowhead) but is absent in mutant tubules (N); arrows show staining of whole nucleus of spermatocytes. For E and F, a minimum of 6 animals were analyzed for each genotype. Results are mean ± SEM, *** p < 0.0001 versus controls. Scale bars = 20 μm.

cytes (whole nucleus staining, arrows) and few sparse pachytene spermatocytes (punctate staining, arrowheads) within Δ/Y testis (J) compared to wild type (I). Few metaphasic cells are also present in *Gilz* mutants as shown by histone H3Ser10 phosphorylated (pH3) positive cells (compare staining in K and L). M, N Sex chromatin of round spermatids is detected by punctate H3K9Me3 staining in control tubules (M, arrowhead) but is absent in mutant tubules (N); arrows show staining of whole nucleus of spermatocytes. For E and F, a minimum of 6 animals were analyzed for each genotype. Results are mean ± SEM, *** p < 0.0001 versus controls. Scale bars = 20 μm.

seminiferous epithelium disorganization, absence of spermatozoa and complete sterility (online suppl. fig. 5G–L). These observations, together with the GILZ expression profile we described above, led us to conclude that the phenotype observed in the constitutive mutants was the exclusive result of an intrinsic germ cell failure,

rather than defects in Sertoli cell or Leydig cell function. Since both the constitutive *Gilz*^{Δ/y} and the germ cell-specific *Gilz* mutant lines are equivalent in terms of reproductive phenotype, we decided to complete the characterization of the phenotype using the constitutive *Gilz*^{Δ/y} line exclusively.

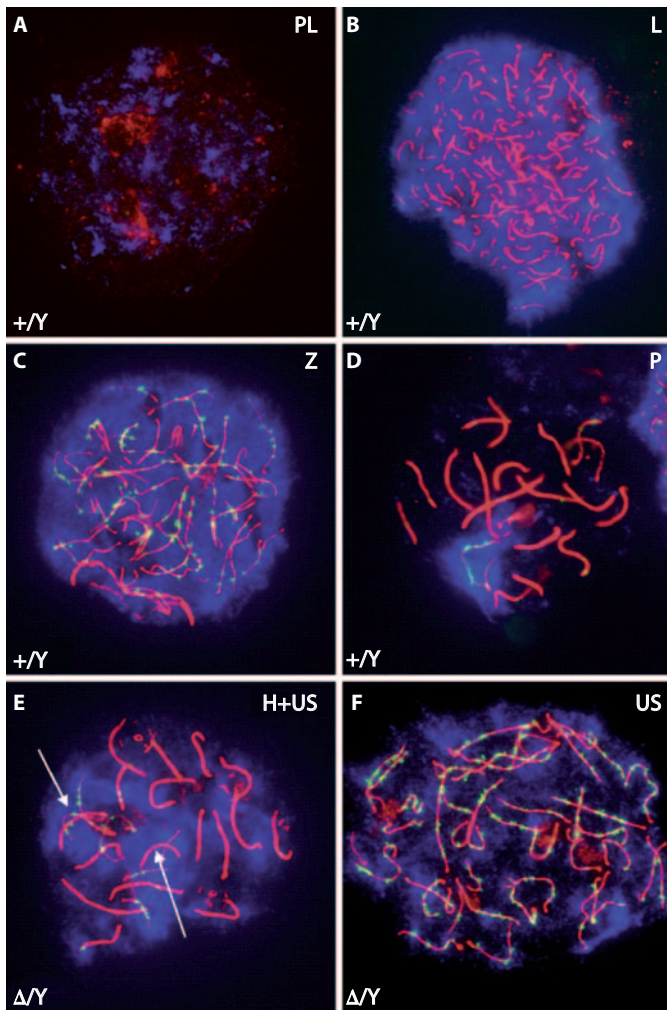


Fig. 3. Meiotic arrest in mid-late zygotene stage in *Gilz^{Δ/y}* mutant testes. Anti-SYCP3 (red), DMC1 (green) and γ H2AX (blue) staining of chromosomal spread preparations from control (+/Y, **A–D**) and mutant (Δ/Y , **E, F**) P12 testes was used to analyze meiotic prophase I cells. Mutant spermatocytes progressed normally from preleptotene to late zygotene and early pachytene. They showed a distinct γ H2AX signal from preleptotene to zygotene all over the nucleus, and in pachytene the expected signal was restricted to the sex body. This suggests that double strand breaks are formed normally. DMC1 (meiotic Rad51 homolog) is recruited to the axis in zygotene, suggesting that repair is initiated. Mutant spermatocytes also revealed a significantly higher amount of nuclei showing a complete set of unsynapsed chromosomes (US) or nuclei containing both, unsynapsed (arrows) and homogenously synapsed chromosomes (H+US). PL, preleptotene; L, leptotene; Z, zygotene; P, pachytene.

*Meiotic Progression Defects and the Absence of Late Meiotic and Post-Meiotic Germ Cells in *Gilz^{Δ/y}* Mutant Mice*

Histological analyses and immunohistochemistry using several germ cell-specific antibodies revealed severely impaired spermatogenesis in P80 *Gilz^{Δ/y}* mice. First, anti-GCNA staining indicated that germ cells are drastically reduced in mutant tubules compared to control littermates, with the majority of seminiferous tubules being Sertoli cell-only tubules (fig. 2G, H). The few remaining germ cells found in *Gilz^{Δ/y}* testes display the morphological features of spermatogonia and early spermatocytes. By using γ H2AX immunostaining, which discriminates between leptotene/zygotene spermatocytes (nuclear staining) and pachytene spermatocytes (γ H2AX sex body punctate staining), we found that the majority of the remaining germ cells in P80 *Gilz^{Δ/y}* testis were spermatocytes in the early prophase I stage (fig. 2I, J). On the other hand, exfoliating pachytene spermatocytes were only sparsely detected in the lumen of degenerating tubules, and metaphasic germ cells were very rarely found (pH3 staining, fig. 2K, L).

As expected, spermatozoa were never found in the tubules' lumen due to a complete absence of round spermatids. This was confirmed by the absence of round spermatid sex chromatin staining in H3K9Me3 immunolabelled mutant testis sections (fig. 2M, N).

To identify at which precise stage the progression of meiotic prophase I is affected in *Gilz^{Δ/y}* mutant animals, we performed anti-SYCP3, DMC1 and γ H2AX staining of chromosomal spread preparations from germ cells collected at P12. While spermatocytes at the preleptotene, leptotene and zygotene stages were present, we observed a drastic reduction in the number of pachytene spermatocytes in mutant testes, suggesting an arrest at mid-late zygotene stage (fig. 3A–D). Differences in the meiotic process were also observed in mutant germ cells, with abnormally high levels of asynapsis found in leptotene and zygotene spermatocytes (fig. 3E, F). In contrast, DNA repair (DMC1 punctate staining) was not affected.

*Spermatogenic Defects Appear as Early as P5 in *Gilz^{Δ/y}* Mutant Mice*

In order to detail precisely the chronology of these multiple defects, we compared the development of control and mutant testes from P0 to P21 during the first wave of spermatogenesis. No discernible abnormality was found in mutant testes at birth and at P3 (data not shown and fig. 4A, B). However, the first defects appeared at P5 during the mitotic phase (fig. 4C, D) with a 2-fold

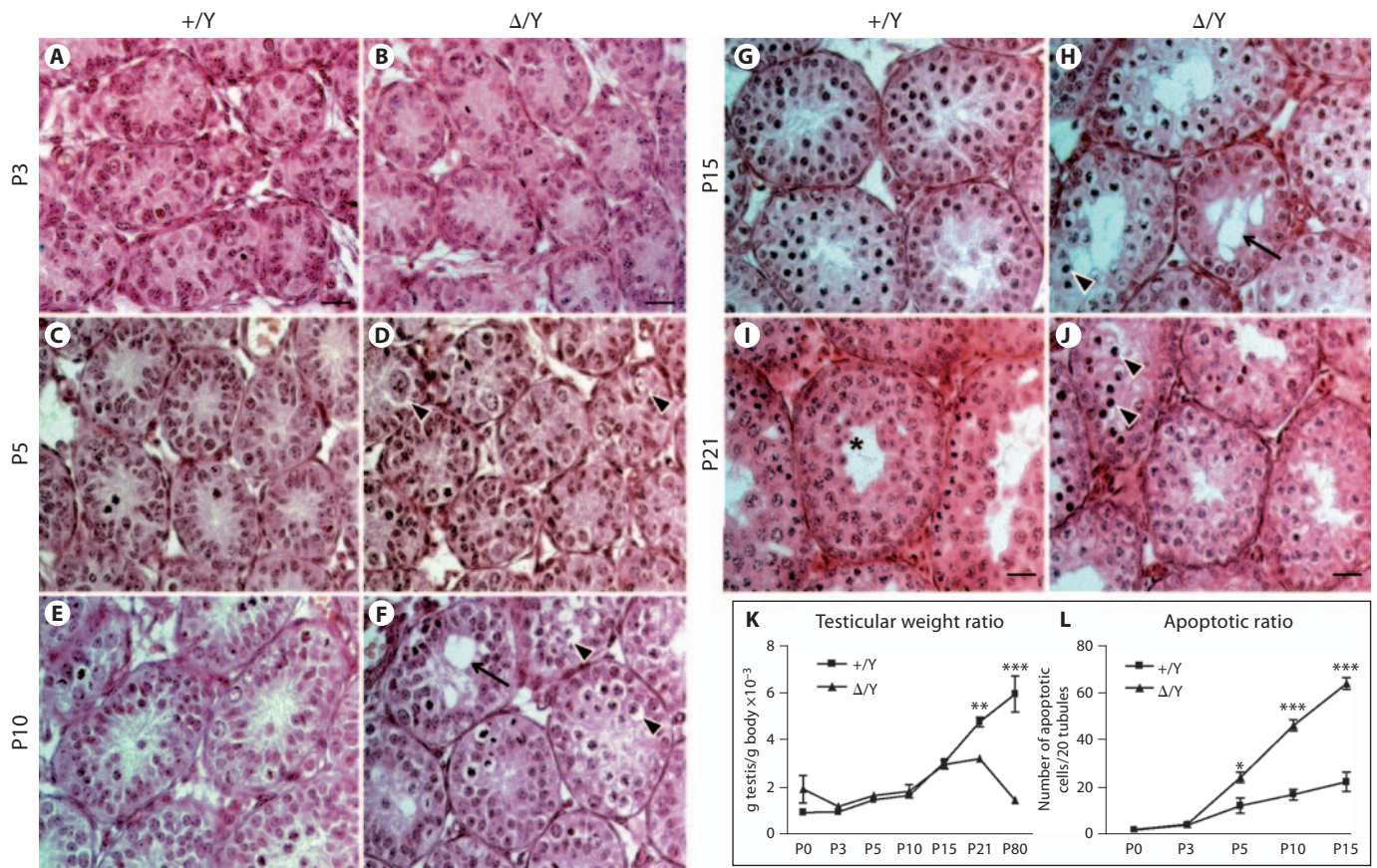


Fig. 4. Tubular defects appear as early as P5 in *Gilz*^{Δ/Y} mice. H&E staining of control (+/Y) (A, C, E, G, I) and mutant (Δ/Y) (B, D, F, H, J) testes at P3 (A, B), P5 (C, D), P10 (E, F), P15 (G, H) and P21 (I, J). The first anatomical defects including apoptosis and germ cell disorganization appeared at P5 (D, arrowheads) and worsened by P10 (F) including vacuolisations (arrow). In P15 and P21 (H, J), tubular histology is strongly affected, with numerous vacuoles

and apoptotic germ cells remaining. In I, the asterisk shows developing round spermatids in the centre of the tubule. Reduced testis weight ratio (K) correlates with an increase in apoptotic rate (L) during the first spermatogenic wave. For K and L, a minimum of 5 animals were analyzed for each genotype. Results are mean ± SEM, * p < 0.05, ** p < 0.01, *** p < 0.001 versus controls. Scale bars = 20 μm.

increase in spermatogonial apoptosis in mutant testes when compared with control individuals (fig. 4L, 24 ± 2 vs. 12 ± 3 apoptotic cells/20 tubules). Moreover, histological analysis suggested that germ cell migration to the base of the epithelium was affected in the mutant mice (fig. 4D, arrowheads). At around P10, when preleptotene spermatocytes normally enter meiosis I, histological abnormalities were more numerous in the mutant mice, with the presence of numerous pycnotic cells, germ cell sloughing (fig. 4F, arrowheads) and the appearance of Sertoli cell cytoplasmic extensions and vacuolisations (fig. 4F, arrow). At this stage, apoptosis was increased by ~3-fold in mutant testes compared to controls (fig. 4L, 46 ± 2 apoptotic cells/20 tubules vs. 17 ± 2 apoptotic

cells/20 tubules). By P15 and P21, these defects were more pronounced (fig. 4G–J). In contrast, spermatogonial proliferation was not affected in mutant testes at P3, P5 and P10 (online suppl. fig. 6). A reduction in mutant testis weight became apparent from P21 onward, due to seminiferous epithelium deterioration and increased apoptosis (fig. 4K, 29 ± 5 mg vs. 58 ± 3 mg and 43 ± 2 mg vs. 219 ± 4 mg, respectively). In P21 control individuals, spermatocytes had undergone meiotic division, and some tubules presented cells in metaphase and haploid round spermatids (fig. 4I, asterisk). At the same stage in mutant animals, however, numerous germ cells were pycnotic, and no round spermatids were found in the seminiferous epithelium (fig. 4). Taken together, these data show that

the loss of *Gilz* severely impairs the first spermatogenic wave, and causes massive apoptosis of spermatogonia, associated higher levels of asynapsis in leptotene and zygotene spermatocytes, and meiotic arrest at the mid-late zygotene stage.

Ablation of Gilz Did Not Cause Alterations in the Testicular Transcriptome at P3

In an attempt to assess the effects of GILZ on gonocyte/prespermatogonia/spermatogonia development at the transcriptional level, we performed a microarray analysis on control and mutant testes at P3, just prior to the first appearance of morphological changes in the mutant mice (P5). At this early postnatal stage, GILZ is already expressed in A spermatogonia (see fig. 1). To our surprise, the expression analysis did not reveal any transcriptional changes in the mutant at this stage, with the notable exception of *Gilz* itself (data not shown).

Discussion

Here we show that *Gilz* is expressed in A and B spermatogonia and early meiotic cells such as preleptotene spermatocytes. To better characterize the role of GILZ in spermatogenesis, we used the Cre/Lox system to ablate *Gilz* either constitutively in whole mice or conditionally in germ cells. While female reproductive functions remained unaffected, male mice lacking functional GILZ, either constitutively or specifically in germ cells, were sterile due to a complete absence of mature spermatozoa. The seminiferous epithelium of adult mutant mice was depleted in germ cells, with the presence of numerous Sertoli cell-only tubules as well as tubules with sparse spermatogonia and primary spermatocytes. A developmental analysis revealed that the first alterations appeared as early as P5. Spermatogenic failure was intrinsic to germ cells in the mutant mice and was associated with massive spermatogonial apoptosis as well as defects in meiotic progression. Collectively, our data show that GILZ is essential for spermatogonia survival and the early phases of meiosis I.

While this manuscript was in preparation, a report was published describing the reproductive phenotype of *Gilz* inactivation in mice [Bruscoli et al., 2012]. Similar to our study, Bruscoli and colleagues generated constitutive and germ cell-specific ablations of *Gilz* using the same *Ddx4:Cre* transgene [Gallardo et al., 2007] to investigate the role of GILZ during spermatogenesis. As expected, their results are overall in agreement with our observa-

tions, including male infertility because of massive apoptosis in the germ cell lineage. We nevertheless observed several divergent results. For example, germ cell loss appeared more severe in their report, with the presence of empty tubules containing only Sertoli cells. In contrast, we found a significant fraction of seminiferous tubules in adult animals (~1/4) that still contained germ cells at both the spermatogonial and early meiotic stages. The differences in the severity of these phenotypes could potentially be explained by differences in genetic background but not by the gene-deletion strategies themselves, as the Cre-mediated deletion of the 2 *Gilz* floxed alleles used in these studies resulted in the complete absence of GILZ protein [Bruscoli et al., 2012; Suarez et al., in press]. Another important difference between the 2 studies relates to apoptosis and proliferation. While we observed no alteration in proliferation at P3, P5 and P10 and the first events of spermatogonial apoptosis at P5, Bruscoli and coworkers measured an increase in proliferation rate of undifferentiated spermatogonia at P7 and an increase in apoptosis only at P10.

In conclusion, the results of our studies clearly identify GILZ as an essential molecule for spermatogonia development and spermatogenesis. GILZ appears to be required for the development of germ cells, particularly during the early steps of spermatogenesis. Its depletion affects spermatogonia survival and potentially differentiation, perhaps leading to subsequent meiotic defects including the inability to complete meiosis I. It remains unclear how GILZ affects the equilibrium between self-renewal, proliferation, differentiation and survival in spermatogonia and furthermore, by which molecular mechanism meiosis is impaired. Clearly more studies are needed to identify the precise functions and signalling pathways regulated by GILZ in spermatogenesis.

Acknowledgements

We would like to thank Chantal Combépine and Nicolas Veillard for excellent technical assistance and Pierre Calvel for critical reading of the manuscript.

References

- Ayroldi E, Zollo O, Macchiarulo A, Di Marco B, Marchetti C, Riccardi C: Glucocorticoid-induced leucine zipper inhibits the Raf-extracellular signal-regulated kinase pathway by binding to Raf-1. *Mol Cell Biol* 22:7929–7941 (2002).
- Ayroldi E, Zollo O, Bastianelli A, Marchetti C, Agostini M, et al: GILZ mediates the anti-proliferative activity of glucocorticoids by negative regulation of Ras signaling. *J Clin Invest* 117:1605–1615 (2007).
- Bruscoli S, Velardi E, Di Sante M, Bereshchenko O, Venanzi A, et al: Long-glucocorticoid-induced leucine zipper (L-GILZ) interacts with Ras pathway and contributes to spermatogenesis control. *J Biol Chem* 287:1242–1251 (2012).
- Chalmel F, Rolland AD, Niederhauser-Wiederkehr C, Chung SS, Demougin P, et al: The conserved transcriptome in human and rodent male gametogenesis. *Proc Natl Acad Sci USA* 104:8346–8351 (2007).
- Cohen N, Mouly E, Hamdi H, Maillot MC, Pallardy M, et al: GILZ expression in human dendritic cells redirects their maturation and prevents antigen-specific T lymphocyte response. *Blood* 107:2037–2044 (2006).
- D'Adamio F, Zollo O, Moraca R, Ayroldi E, Bruscoli S, et al: A new dexamethasone-induced gene of the leucine zipper family protects T lymphocytes from TCR/CD3-activated cell death. *Immunity* 7:803–812 (1997).
- Delfino DV, Agostini M, Spinicelli S, Vito P, Riccardi C: Decrease of Bcl-xL and augmentation of thymocyte apoptosis in GILZ overexpressing transgenic mice. *Blood* 104:4134–4141 (2004).
- de Rooij DG: The spermatogonial stem cell niche. *Microsc Res Tech* 72:580–585 (2009).
- de Rooij DG, de Boer P: Specific arrests of spermatogenesis in genetically modified and mutant mice. *Cytogenet Genome Res* 103:267–276 (2003).
- Gallardo T, Shirley L, John GB, Castrillon DH: Generation of a germ cell-specific mouse transgenic Cre line, *Vasa-Cre*. *Genesis* 45:413–417 (2007).
- Grad I, Cederroth CR, Walicki J, Grey C, Barluenga S, et al: The molecular chaperone Hsp90alpha is required for meiotic progression of spermatocytes beyond pachytene in the mouse. *PLoS One* 5:e15770 (2010).
- Krzysiek R: Role of glucocorticoid-induced leucine zipper (GILZ) expression by dendritic cells in tolerance induction. *Transplant Proc* 42:3331–3332 (2010).
- Lardenois A, Gattiker A, Collin O, Chalmel F, Primig M: Germonline 4.0 is a genomics gateway for germline development, meiosis and the mitotic cell cycle. *Database (Oxford)* 2010:baq030 (2010).
- Lecureuil C, Fontaine I, Crepieux P, Guillou F: Sertoli and granulosa cell-specific Cre recombinase activity in transgenic mice. *Genesis* 33:114–118 (2002).
- Redjimi N, Gaudin F, Touboul C, Emilie D, Pallardy M, et al: Identification of glucocorticoid-induced leucine zipper as a key regulator of tumor cell proliferation in epithelial ovarian cancer. *Mol Cancer* 8:83 (2009).
- Romero Y, Meikar O, Papaioannou MD, Conne B, Grey C, et al: Dicer1 depletion in male germ cells leads to infertility due to cumulative meiotic and spermiogenic defects. *PLoS One* 6:e25241 (2011).
- Shi X, Shi W, Li Q, Song B, Wan M, et al: A glucocorticoid-induced leucine zipper protein, GILZ, inhibits adipogenesis of mesenchymal cells. *EMBO Rep* 4:374–380 (2003).
- Soundararajan R, Zhang TT, Wang J, Vandewalle A, Pearce D: A novel role for glucocorticoid-induced leucine zipper protein in epithelial sodium channel-mediated sodium transport. *J Biol Chem* 280:39970–39981 (2005).
- Soundararajan R, Wang J, Melters D, Pearce D: Differential activities of glucocorticoid-induced leucine zipper protein isoforms. *J Biol Chem* 282:36303–36313 (2007).
- Suarez P, Rodriguez EG, Soundararajan R, Merrillat AM, Stehle JC, et al: The glucocorticoid-induced leucine zipper (*Gilz/Tsc22d3-2*) gene locus plays a crucial role in male fertility. *Mol Endocrinol*, in press.
- Zhou Q, Griswold MD: Regulation of Spermatogonia (Stembook, Cambridge 2008).